Geoelectrical Survey for Groundwater at the
Gidan Kwano Campus of the Federal University of Technology, Minna

Udensi, E.E.,*Unuevho, C.I., Jonah, S.A., Ofor, P.N., Adetona, A.A., Salako, K.A., Gana, C.S., Nwosu, J.E., Mulero, E.O., Iwuafor, H.O., Akinloye, O.A., and Owolabi, E.O.

Department of Physics, Federal University of Technology, Minna, Nigeria.
* Department of Geology, Federal University of Technology, Minna, Nigeria.

Abstract

A 1km x 1/2 km grid geoelectrical resistivity survey using the Schlumberger (i.e. sounding) mode was conducted in the swath of land between the Staff Quarters and the temporary Administration/Hostel blocks stretching to just the edge of the new School of Engineering and Engineering Technology (S.E.E.T.) complex. The purpose of the survey was to primarily determine electrically the horizons or formations, of their thickness, including relative positions and depths under the surface. Sixty-six VES stations were occupied, and the data collected were reduced and subjected to n-layer model analysis by Zohdy technique. The results of this analysis are presented as curves of different resistivity versus depth. From the digitized curves, iso-resistivity maps at different depth, and geoelectric vertical section of each profile were obtained. The results show that VES points B2, C4, E2, G3, I4, J3, J6, K3, and K6 are the points identified as suitable for drilling boreholes for the purpose of water exploitation.

Keywords: Geoelectrical, VES, resistivity, aquifer, overburden

1.0 Introduction

Nearly everyone will agree that mankind, at this point in time more than ever before, is saddled with the critical responsibility of sustainably managing the earth's resources that are beginning to show signs of decline. Water is one of such very important resources, and thus the search for underground water sources as supplements to the surface water sources to meet the demand of a burgeoning population is central to government policies and scientific endeavours. In science, this search is encompassed in the earth sciences' disciplines of geology and applied geophysics. Geophysical prospecting for underground aquifers is often vexed by the problem of data resolution, although the availability of these data in the first place is a function of the availability of modern field surveying equipment which can be expensive indeed. Another constraint is the non-availability of a large spread of data over developed areas that would provide several options for drilling programmes in area where the local geology may not be too favourable for large scale existence of aquifer systems.

This exercise is a follow-up of previous attempts to determine groundwater potentials, the principal objective being the identification of suitable sites for exploitation of groundwater by drilling of boreholes around developed areas of the Gidan Kwano Campus (Udensi et al., 2005; Salako & Udensi, 2005). This study was carried out in the area of land between the University's Staff Quarters and the temporary Administrative/Hostel blocks. It is imperative to continuously locate viable aquifers in order to meet the rise in demand occasioned by the phased movement to the Gidan Kwano Campus of the administrative and academic activities of the Federal University of Technology, Minna. This study aims to improve the overall aquifer database of the Federal University of Technology, Minna, because a recent large scale drilling scheme was fraught with less than expected success.

1.1 Locations of Gidan Kwano Campus

The Gidan Kwano Campus of the Federal University of Technology, Minna, is located along the Minna-Bida road. The site is about 10,600 hectares in areal extent and it lies between latitude $9^0 26^1 15^{11}$ and $9^0 37^1 30^{11}$N and longitude $6^0 21^1 15^{11}$ and $6^0 28^1 45^{11}$E. It has the shape of a bow, bulging out from the centre towards the east and stretching the upper arm towards the northwest at about 45^0 and the lower arm to the southwest at about the same angle (Udensi et al., 2005).

1.2 Geology of Gidan Kwano Campus

The area is underlain by Basement Complex rocks consisting of medium-grained biotite granite interbanded with coarse-grained leucocratic granite and intruded in places by quatzo-feldspar pegmatite dykes. The dykes strike parallel to the strike of the foliation, and they range from 0.5m to 3.5m in diameter. Outcrops are found along the river valleys as flat-lying bodies. They range in sizes from 3x5m to about 8x15m. Pinkish feldspar (i.e potassium feldspar) is the dominant mineral in the granite gneiss and the pegmatite. This implies that its weathered product will be rich in clay.

The rock types found here are believed to be part of older granite suite and are mostly exposed along the river channels where they appear in most cases weathered. Based on the relative grain size, the major rock types are (i)

Geoelectrical Survey for Groundwater at the Gidan Kwano Campus of the Federal University of Technology, Minna- Udensi et al

16

porphyritic coarse-grained granite, and (ii) medium to fine-grained granites. The former are mostly flat-lying with sizes ranging from few metres to about thirty metres. They are believed to continuously underlay the region that is covered by the thick overburden and are found outcropping along the river channels. Owing to biological weathering, the outcrops are broken into boulders (Salako and Udensi, 2005). The latter are also flat-lying along the river channels and relatively high rising elongated outcrops on the surface, and unlike the pophyritic granite they are less weathered. The rocks are found in East-West (E-W) treading veins and joints which are sometimes filled by aplitic or quartz; this is in contrast to the porphyritic granite that are found in the North-South (N-S) trending quarts and aplitic veins ranging in length from 2m to about 15m. The medium to fine-grained granitic rocks are broken up into boulders in some places and they show the effect of weathering in the form of colour change, and loose rock fragments.

2.0 The Geoelectric Survey
2.1 Project Location:
The geophysical survey covered an area of 1000m x 500m. The area is bounded on the east extending for 1km by the male hostel, the temporary administrative block, and the water storage facility just northeast of the new SEET complex. To the west is the Staff Quarters and the expanse of land just south of the Staff Quarters. To the south of the survey area is a tarred motor way and to the north are cultivated farmlands.

2.2 The Method Employed
The geophysical work carried out here is based on electrical resistivity survey using the vertical electrical sounding (VES) technique (Parasnis, 1986; Kearey and Brooks, 1988). Generally, an electrical resistivity method involves the artificial introduction of current into the ground through points electrodes. Potentials are subsequently measured at other electrodes in the vicinity of the current flow. By this means, it is then possible to measure or determine an effective or apparent resistivity of the subsurface. Low resistivity in a given area is a likely indicator of the presence of groundwater (Ako and Olorunfemi, 1982; Gana, 1995; Bonde, 1997; Dangana, 2002). The VES determine the vertical sequence of the underlying strata (Olorunfemi and Okhue, 1992; Okwueze et al, 1981; Okwueze and Ezeanyi, 1985; Olorunfemi and Fasuyi, 1993; Shuaibu et al, 2004). The Schlumberger array or configuration was employed in the VES investigation of the area surveyed.

In the Schlumberger configuration the current and potential pairs of electrodes have a common mid-point but the distance between adjacent electrodes differs. Let the separations of the current and potential electrodes be L and a respectively, it then follows that

$$T_{AM} = T_{NB} = \frac{(L-a)}{2} \tag{1}$$

$$T_{AM} = T_{MB} = \frac{(L+a)}{2} \tag{2}$$

$T_{AM}, T_{NB}, \quad T_{MB}$ are specific ratios of the separations between the current and potential electrodes.

If these quantities are substituted into the general expression for the resistivity of the four-electrode method,

$$\rho = 2\pi \frac{v}{II} \left[\frac{1}{\left(\frac{1}{T_{AM}} - \frac{1}{T_{MB}} \right) - \left(\frac{1}{T_{AM}} - \frac{1}{T_{AB}} \right)} \right]$$

we obtain the resulting expression

i.e

$$\rho = 2\pi \frac{v}{I} \left[\frac{1}{\left(\frac{2}{L-a} - \frac{2}{L+a} \right) - \left(\frac{2}{L+a} - \frac{2}{L-a} \right)} \right]$$

Progressively increasing the distance

or

$$\rho = \frac{\pi}{4} \frac{v}{I} \left[\frac{L^2 - a^2}{a} \right] \tag{3}$$

between adjacent electrodes of the Schlumberger configuration will cause the current lines to penetrate to ever greater

Geoelectrical Survey for Groundwater at the Gidan Kwano Campus of the Federal University of Technology, Minna- Udensi et al

17

depth depending on the vertical distribution through A and B. The magnitude of the potential difference developed was a measure of the electrode spacing MN; this resistance is a function of the geometrical configuration and the electrical parameters of the ground (Bhattacharya, 1986).

As the current electrode spacing AB gets larger, the potential difference between MN decreased rapidly and becomes negligibly below the measuring capability of the instruments. This is because the field at the center of the configuration normally varies inversely as the square of the length of the configuration AB. The common field practice is that the separation of the potential electrodes should be increased such that the new value is larger than the preceding value. Using this procedure, sixty-six (66) vertical electrical soundings were carried out.

3.0   Data Collection:

The SAS4000/SAS1000 resistivity meter (manufactured by ABEM of Sweden) measures the potential due to an appropriately selected (else the equipment automatically selects a default current value) current value and displays the computed value of resistance. The raw data recorded is the resistance (R) of the ground and the half-current electrode separation. This resistance multiplied by the geometrical configuration factor gives the apparent resistivity (ρ) of the ground. It follows therefore, that the value of the apparent resistivity obtained depends on electrode array band the distribution of the resistivity in the earth. Sixty six (66) VES stations were occupied and about one thousand three hundred and eighty six (1386) data set were collected over a period of two weeks; a 1km x 1/2 km survey at 100m intervals gives 66 (6 x 11) VES points. The maximum AB spread at each VES point is 200m (i.e AB/2 = 100m), resulting in 21 recorded values of the resistance (R) at each VES point, thus a total of 126 (21x6) data set were recorded for each of the eleven profiles. This translated to 1386 (12 x 11) data set in all. The complete dataset for Profiles A-K are shown in the Appendix. Logistics difficulties precluded the exact determination in terms of their appropriate coordinate points of each of the 66 stations occupied.

3.1   Data Analysis

The data collected were first processed by smoothing and using an iterative computer program called the Zohdy Graphical Method. This program performs automatic interpretation of both curves that is used to obtain the equivalent multi- or n-layer model from the apparent resistivity curve of each sounding (Zohdy, 1989). The field curves were obtained by plotting the apparent resistivity against half-current electrode spacing on a bi-logarithmic or log-log graph paper. The analysis of the apparent resistivity variation at different electrode spacing makes it possible to draw conclusions about the subsurface.

3.2   Interpretation

Resistivity values can be presented in the form of a depth curve, a profile or contour map. The apparent resistivity curve for layer structure has typical shapes determined by the vertical sequence of resistivities in the layers.

3.3   The Continuous Variation of Resistivity with Depth

A continuous variation of resistivity with depth curve is easily derived from multilayer step-function curve by drawing a curve that passes through the logarithmic midpoint of each vertical and horizontal line on the multilayer step function model. In view of the fact that the layer depths are logarithmically closely-shaped, the derived continuous variation of resistivity with depth model is equivalent to the original model. This approach makes it easy to construct maps of contoured resistivity values at different depths and to construct contoured geoelectric sections.

4.0   Vertical Electrical Depth Sounding Results

The summaries of the results deduced from the digitized Zohdy curves derived from the interpretation of the VES field data set are presented in Tables 1-11. The interpretation of the layering of Table 1 shows that VES points A2, A3, A4, A5, and A6 are made up of five geoelectric units or layers: there are six layers for VES point A1. Along profile A, the resistivity of the uppermost layer (topsoil) varies from a low of 0.70 Ωm (for A6) to a high of 241.62 Ωm (for A1).

The resistivity extreme in this profile has its highest value of 3562.62Ωm in the first layer underneath VES point A3. The second and third layers underneath VES A3 also show very high resistivity. The lowest resistivity value of 0.18Ωm occurs in the second layer underneath VES A5. The thickest layer that can be deduced from this profile is 17.74m, and this is the thickness of the fourth layer of VES A2 and also the thickness of the fourth layer of VES A6. The thinnest layer corresponds to the first layer of both VES points A4 and A5. The thickness of the top layer remains fairly constant in this profile (from 0.40m to 0.54m). Finally the depth to basement along this profile varies from 26.82m to 36.79m.

Geoelectrical Survey for Groundwater at the Gidan Kwano Campus of the Federal University of Technology, Minna- Udensi et al

18

Table 1: Summary of VES Interpretation of Profile A.

VES POINT	LAYER NUMBER	AVERAGE RESISTIVITY (Ωm)	DEPTH (m)	LAYER THICKNESS (m)
A1	1	241.622	0.000	0.540
	2	35.730	0.540	0.623
	3	371.271	1.163	10.471
	4	834.452	11.634	13.431
	5	281.012	25.065	11.725
	6	140.696	36.790	∞
A2	1	138.296	0.000	0.486
	2	83.004	0.486	0.561
	3	90.969	1.047	14.322
	4	504.695	15.369	17.742
	5	656.124	33.111	∞
A3	1	3562.622	0.000	0.437
	2	1525.881	0.437	0.946
	3	1232.681	1.383	12.449
	4	118.591	13.832	15.968
	5	205.476	29.800	∞
A4	1	1.871	0.000	0.394
	2	2.381	0.394	0.851
	3	2.946	1.245	11.204
	4	1.723	12.449	14.371
	5	26.633	26.820	∞
A5	1	6.336	0.000	0.394
	2	0.182	0.394	0.851
	3	0.461	1.245	11.204
	4	3.568	12.449	14.371
	5	46.451	26.820	∞
A6	1	0.704	0.000	0.486
	2	1.219	0.486	0.561
	3	2.677	1.047	14.322
	4	2.279	15.369	17.742
	5	23.283	33.111	∞

Table 2: Summary of VES Interpretation of Profile B

VES POINT	LAYER NUMBER	AVERAGE RESISTIVITY (Ωm)	DEPTH (m)	LAYER THICKNESS (m)
B1	1	979.7085	0.000	0.540
	2	345.526	0.540	0.623
	3	236.106	1.163	10.471
	4	2,885.152	11.634	13.431
	5	11,969.870	25.065	11.725
	6	69,419.51	36.790	∞
B2	1	57.513	0.000	0.540
	2	34.746	0.540	0.623
	3	20.285	1.163	10.471
	4	70.243	11.634	13.431
	5	311.345	25.065	11.725
	6	1,998.105	36.790	∞
B3	1	4.865	0.000	0.520
	2	13.167	0.520	0.600
	3	30.943	1.120	10.084
	4	197.619	11.204	12.934
	5	1,237.740	24.138	∞
B4	1	6.848	0.000	0.486
	2	0.458	0.486	0.561
	3	57.215	1.047	14.322
	4	448.833	15.369	17.742
	5	730.197	33.111	∞
B5	1	36.792	0.000	0.642
	2	11.341	0.642	0.741
	3	28.031	1.383	12.449
	4	263.419	13.832	15.968
	5	1,925.988	29.800	∞
B6	1	286.598	0.000	0.307
	2	662.972	0.307	1.118
	3	546.021	1.425	12.828
	4	418.040	14.253	∞

The interpretation of Table 2 shows that VES B6 is made up of four geoelectric units or layers, while B3, B4, B5 are made up of five layers, and B1,B6, consists of six geoelectric units. Along this profile, the resistivity of the uppermost layer (topsoil) varies form 4.86 Ωm to 979.71 Ωm; these occur for B1 and B3 respectively. The resistivity extreme in this profile has its highest value of 69,419.51Ωm in the sixth layer underneath VES A1. The fifth layer of VES A1 also shows very high resistivity. The lowest resistivity value of 0.46Ωm occurs in the second layer underneath VES B4. The thickest layer seen in this profile is 17.74m, and this occurs for the fourth profile of VES B4 while the thinnest layer of 0.31m corresponds to the top layer of VES B6. The thickness of the top layer does not vary too much as this range from 0.31m to 0.64m. Finally, the depth to basement along this profile varies from 14.25m to 36.79m; it is shallow at B6 and deepest at B1.

Table 3 shows that C1 is made up of four layers, VES C2 is made up of five layers, and VES C3, V4, C5 and C6 are made up of six geoelectric units or layers each. The highest resistivity value if 51,010.73 Ωm occurs at the sixth layer of VES C6 while the lowest resistivity value of 0.14Ωm occurs at the second layer of VES C4. The thickest layer of 17.7m occurs as the fourth layer of VES C2 while the thinnest layer of 0.26m is the first layer of VES C1. The thickness of the first or topmost layer varies from 0.26m (for C1) to 0.54m (for C3, C4, C5 and C6). The basement on this profile is deepest under VES points C3, C4, C5 and C6, and thinnest under VES C1.

Geoelectrical Survey for Groundwater at the Gidan Kwano Campus of the Federal University of Technology, Minna- Udensi et al

19

Table 3: Summary of VES Interpretation of Profile C.

VES POINT	LAYER NUMBER	AVERAGE RESISTIVITY (Ωm)	DEPTH (m)	LAYER THICKNESS (m)
C1	1	90.247	0.000	0.258
	2	155.533	0.258	0.941
	3	38.325	1.199	16.397
	4	1988.654	17.596	∞
C2	1	1055.991	0.000	0.486
	2	708.954	0.486	0.561
	3	566.895	1.047	14.322
	4	692.100	15.369	17.742
	5	503.391	33.111	∞
C3	1	2.752	0.000	0.540
	2	0.785	0.540	0.623
	3	101.304	1.163	10.471
	4	798.983	11.634	13.431
	5	2096.759	25.065	11.725
	6	6673.330	36.790	∞
C4	1	0.328	0.000	0.540
	2	0.140	0.540	0.623
	3	2.545	1.163	10.471
	4	30.533	11.634	13.431
	5	84.152	25.065	11.725
	6	325.537	36.790	∞
C5	1	1080.029	0.000	0.540
	2	2223.579	0.540	0.623
	3	18703.851	1.163	10.471
	4	7870.168	11.634	13.431
	5	404.9637	25.065	11.725
	6	821.305	36.790	∞
C6	1	150.194	0.000	0.540
	2	41.630	0.540	0.623
	3	344.988	1.163	10.471
	4	4928.515	11.634	13.431
	5	14342.300	25.065	11.725
	6	51010.725	36.790	∞

Table 4: Summary of VES Interpretation of Profile D

VES POINT	LAYER NUMBER	AVERAGE RESISTIVITY (Ωm)	DEPTH (m)	LAYER THICKNESS (m)
D1	1	26.474	0.000	0.486
	2	40.5891	0.486	0.561
	3	145.594	1.047	14.322
	4	253.987	15.369	17.742
	5	472.880	33.111	∞
D2	1	20.875	0.000	0.437
	2	21.856	0.437	0.946
	3	70.042	1.383	12.449
	4	144.485	13.832	15.968
	5	306.063	29.800	∞
D3	1	43.245	0.000	0.540
	2	34.066	0.540	0.623
	3	48.150	1.163	10.471
	4	779.190	11.634	13.431
	5	2322.486	25.065	11.725
	6	4666.670	36.790	∞
D4	1	30.974	0.000	0.540
	2	17.361	0.540	0.623
	3	30.000	1.163	10.471
	4	439.846	11.634	13.431
	5	1175.203	25.065	11.725
	6	2955.806	36.790	∞
D5	1	79.163	0.000	0.394
	2	96.138	0.394	0.851
	3	155.019	1.245	11.204
	4	529.661	12.449	14.371
	5	1294.288	26.820	∞
D6	1	272.968	0.000	0.486
	2	245.060	0.486	0.561
	3	120.595	1.047	14.322
	4	215.682	15.369	17.742
	5	438.387	33.111	∞

It is seen in Table 4 that VES points D1, D2, D5 and D6 have five layers each while VES points D3 and D4 are composed of six layers each. Overall, it is seen that the resistivity distribution in this profile generally increase with depth. The highest resistivity value of 4666.6Ωm occurs for the sixth layer of VES D3 while the lowest resistivity of 17.36Ωm occurs for the second layer of VES D4. The thickest layer of 17.74Ωm is found at the fourth layers of VES points D1 and D6 respectively. The deep basement on this profile is underneath VES points D3 and D4 respectively, while the basement is shallow underneath VES point D5.

Table 5 indicates that there are five geoelectric units each underneath the different VES points. The thickness of the top soil is fairly constant, with not too significant variation (from 0.35m to 0.49m). The highest resistivity value of 2735.14Ωm occurs at the fifth layer of E5 while the lowest value of 4.86Ωm occurs at the second layer of E2. The thickest layers of 17.74Ωm are seen as the fourth geoelectric unit underneath E3 and E6. The thickest layer of 0.35m is the top soil of VES point E1.

Geoelectrical Survey for Groundwater at the Gidan Kwano Campus of the Federal University of Technology, Minna- Udensi et al

20

Table 5: Summary of VES Interpretation of Profile E

VES POINT	LAYER NUMBER	AVERAGE RESISTIVITY (Ωm)	DEPTH (m)	LAYER THICKNESS (m)
E1	1	19.491	0.000	0.354
	2	26.616	0.354	0.766
	3	62.354	1.120	10.084
	4	280.817	11.204	12.934
	5	1747.448	24.138	∞
E2	1	23.718	0.000	0.437
	2	4.856	0.437	0.946
	3	8.576	1.383	12.449
	4	47.493	13.832	15.968
	5	458.084	29.800	∞
E3	1	219.792	0.000	0.486
	2	77.754	0.486	0.561
	3	75.023	1.047	14.322
	4	397.253	15.369	17.742
	5	468.219	33.111	∞
E4	1	71.382	0.000	0.437
	2	111.514	0.437	0.946
	3	111.257	1.383	12.449
	4	1170.516	13.832	15.968
	5	1561.112	29.800	∞
E5	1	62.759	0.000	0.394
	2	56.396	0.394	0.851
	3	107.103	1.245	11.204
	4	719.833	12.449	14.371
	5	2735.144	26.820	∞
E6	1	127.171	0.000	0.486
	2	74.847	0.486	0.561
	3	43.139	1.047	14.322
	4	427.133	15.369	17.742
	5	1095.868	33.111	∞

Table 6: Summary of VES Interpretation of Profile F

VES POINT	LAYER NUMBER	AVERAGE RESISTIVITY (Ωm)	DEPTH (m)	LAYER THICKNESS (m)
F1	1	37.409	0.000	0.437
	2	34.026	0.437	0.946
	3	111.000	1.383	12.449
	4	314.035	13.832	15.968
	5	786.345	29.800	∞
F2	1	0.595	0.000	0.354
	2	0.708	0.354	0.766
	3	15.223	1.120	10.084
	4	150.059	11.204	12.934
	5	1,021.749	24.138	∞
F3	1	38.436	0.000	0.394
	2	120.620	0.394	0.851
	3	163.542	1.245	11.204
	4	270.514	12.449	14.371
	5	2020.481	26.820	∞
F4	1	48510.950	0.000	0.341
	2	15,832.304	0.341	0.738
	3	6,914.036	1.079	14.758
	4	432.029	15.837	∞
F5	1	176.848	0.000	0.642
	2	79.215	0.437	0.741
	3	173.162	1.383	12.449
	4	416.051	13.832	15.968
	5	1462.685	29.800	∞
F6	1	146.902	0.000	0.642
	2	85.702	0.437	0.741
	3	89.960	1.383	12.449
	4	413.131	13.832	15.968
	5	1629.913	29.800	∞

Table 6 indicates that for the VES interpretation for profile F, there are four layers for F4 and five layers each for F1, F2, F3, F4, F5 and F6. The thickest layer of 15.97 occurs for the fourth layer of F1, F5, and F6, while the thinnest layer of 0.34m corresponds to the top soil of F4. It is also observed that the thickness of the topsoil is relatively uniform along the entire profile. The highest resistivity value of 48,510.95Ωm is found at the first layer of F4 and the lowest resistivity value of 0.60Ωm corresponds to the topmost layer of F2. The basement is deepest under E1, F5 and F6; it is the shallowest under F4.

Geoelectrical Survey for Groundwater at the Gidan Kwano Campus of the Federal University of Technology, Minna- Udensi et al

21

Table 7: Summary of VES Interpretation of Profile G

VES POINT	LAYER NUMBER	AVERAGE RESISTIVITY (Ωm)	DEPTH (m)	LAYER THICKNESS (m)
G1	1	4.504	0.000	0.520
	2	34.987	0.520	0.600
	3	76.220	1.120	10.084
	4	455.755	11.204	12.934
	5	2,926.208	24.138	∞
G2	1	26.881	0.000	0.437
	2	32.877	0.642	0.946
	3	54.294	1.383	12.449
	4	366.331	13.832	15.968
	5	4,000.802	29.800	∞
G3	1	72.839	0.000	0.437
	2	92.758	0.437	0.946
	3	87.214	1.383	12.449
	4	146.729	13.832	15.968
	5	760.472	29.800	∞
G4	1	90.135	0.000	0.394
	2	22.304	0.394	0.851
	3	77.230	1.245	11.204
	4	824.316	12.449	14.371
	5	4,392.135	26.820	∞
G5	1	15.753	0.000	0.437
	2	82.392	0.437	0.946
	3	75.548	1.383	12.449
	4	406.074	13.832	15.968
	5	1,066.232	29.800	∞
G6	1	5.469	0.000	0.468
	2	16.847	0.468	0.540
	3	5.700	1.008	9.075
	4	52.218	10.083	11.641
	5	347.674	21.724	∞

Table 8: Summary of VES Interpretation of Profile H

VES POINT	LAYER NUMBER	AVERAGE RESISTIVITY (Ωm)	DEPTH (m)	LAYER THICKNESS (m)
H1	1	441.692	0.000	0.642
	2	88.659	0.642	0.741
	3	101.071	1.383	12.449
	4	689.818	13.832	15.968
	5	2,663.238	29.800	∞
H2	1	74.163	0.000	0.486
	2	78.168	0.486	0.561
	3	111.902	1.047	9.424
	4	350.448	10.471	22.64
	5	464.549	33.111	∞
H3	1	39.673	0.000	0.642
	2	64.253	0.578	0.741
	3	41.927	1.245	12.449
	4	125.935	12.449	15.968
	5	1,513.353	26.820	∞
H4	1	8.849	0.000	0.578
	2	44.866	0.578	0.667
	3	47.000	1.245	11.204
	4	190.936	12.449	14.371
	5	817.123	26.820	∞
H5	1	119.301	0.000	0.642
	2	60.871	0.642	0.741
	3	112.686	1.383	12.449
	4	960.336	13.832	15.968
	5	1,742.906	29.800	∞
H6	1	2.632	0.000	0.540
	2	1.181	0.540	0.623
	3	4.641	1.163	10.471
	4	71.701	11.634	13.431
	5	225.759	25.065	11.725
	6	908.805	36.790	∞

It can be inferred from Table 7 that all of the VES points are made up of five layers each. The thickest layer of 15.97Ωm occurs for the fourth layer of G2, the fourth layer of G3, and the fourth layer of G5 while the thinnest layer occurs for the top layer of G6. The highest resistivity value of 4,391 corresponds to the fifth layer of G4; the lowest resistivity value of 4.5Ω corresponds to the first layer of G1. The basement is deep under G2, G3, G3 and it is shallow under G6.

In Table 8, VES points H1, H2, H3, H4, H5 are each characterized by five layers whereas VES points H6 is made up of six layers. The thickest layer of 22.64m occurs as the fourth layer of H2 while the thinnest layer of 0.49m occurs at the top layer of H2. The highest resistivity value of 2,663.24Ωm occurs for the fifth layer of H1 and the lowest resistivity value of 1.19Ωm occurs for the second layer of H6. Generally, apart form the top layer of H1, H5 and H6 it is seen that the resistivity distribution increases with depth. The basement is deepest underneath H2 and shallowest underneath H6.

Geoelectrical Survey for Groundwater at the Gidan Kwano Campus of the Federal University of Technology, Minna- Udensi et al

22

Table 9: Summary of VES Interpretation of Profile I

VES POINT	LAYER NUMBER	AVERAGE RESISTIVITY (Ωm)	DEPTH (m)	LAYER THICKNESS (m)
I1	1	443.197	0.000	0.642
	2	88.915	0.642	0.741
	3	100.821	1.383	12.449
	4	686.192	13.832	15.968
	5	2,651.721	29.800	∞
I2	1	17.507	0.000	0.520
	2	21.326	0.520	0.600
	3	75.495	1.120	10.084
	4	572.773	11.204	12.934
	5	3,837.298	24.138	∞
I3	1	281.346	0.000	0.486
	2	130.631	0.486	0.561
	3	73.079	1.047	9.424
	4	485.261	10.369	22.640
	5	1,094.986	33.111	∞
I4	1	21.627	0.000	0.578
	2	56.748	0.578	0.667
	3	40.034	1.245	11.204
	4	206.740	12.449	14.371
	5	728.074	26.820	∞
I5	1	346.650	0.000	0.642
	2	33.862	0.642	0.741
	3	788.633	1.383	12.449
	4	1,163.820	13.832	15.968
	5	1,614.543	29.800	∞
I6	1	2.178	0.000	0.486
	2	2.364	0.486	0.561
	3	5.359	1.047	9.424
	4	154.580	10.369	22.640
	5	1,376.002	33.111	∞

Table 10: Summary of VES Interpretation of Profile J

VES POINT	LAYER NUMBER	AVERAGE RESISTIVITY (Ωm)	DEPTH (m)	LAYER THICKNESS (m)
J1	1	191.565	0.000	0.642
	2	260.423	0.642	0.741
	3	147.486	1.383	12.449
	4	1271.480	13.832	15.968
	5	2242.948	29.800	∞
J2	1	177.213	0.000	0.642
	2	49.777	0.642	0.741
	3	91.725	1.383	12.449
	4	382.874	13.832	15.968
	5	1,828.193	29.800	∞
J3	1	62.718	0.000	0.642
	2	23.304	0.642	0.741
	3	47.591	1.383	12.449
	4	183.335	13.832	15.968
	5	629.390	29.800	∞
J4	1	12.714	0.000	0.486
	2	13.755	0.486	0.561
	3	10.669	1.047	9.424
	4	139.952	10.369	22.640
	5	1521.070	33.111	∞
J5	1	12.445	0.000	0.486
	2	5.598	0.486	0.561
	3	3.704	1.047	9.424
	4	68.333	10.369	22.640
	5	748.143	33.111	∞
J6	1	3.504	0.000	0.540
	2	1.576	0.540	0.623
	3	0.641	1.163	10.471
	4	6.654	11.634	13.431
	5	21.962	25.065	11.725
	6	90.680	36.790	∞

There are five layers each underneath I1, I2, I3, I4, I5 and I6 as seen in Table 9. The thickest layers are underneath I3 and I6 and incidentally, the thickest layers are the top layer of I3 and I6. The highest resistivity value of 3837.30Ωm occurs at the first layer of I2 and the lowest resistivity value of 2.18Ωm occurs at the top layer of I6. The basement is deepest under I3 and I6 and it is shallowest under I2.

In Table 10 there are five geoelectric units or layers each for J1, J2, J3, J4 and J5; only VES point J6 has six layers. The thickest layer of 22.64m corresponds to the fourth layer of J4 and J5 and the thinnest layer of 0.49m corresponds to the top layer of J4 and J5. The value of 2242Ωm, which is the highest resistivity, occurs at the fifth layer of J1 and the lowest resistivity of 0.6Ωm occurs at the third layer of J6. The basement is deepest underneath J6 and shallowest underneath J1, J2, and J3.

Geoelectrical Survey for Groundwater at the Gidan Kwano Campus of the Federal University of Technology, Minna- Udensi et al

23

Table 11: Summary of interpretation of profile K

VES Point	Layer Number	Average resistivity (Ωm)	Depth (m)	Layer thickness (m)
K₁	1	123.610	0.000	0.642
	2	217.911	0.642	0.741
	3	141.767	1.393	12.449
	4	1014.282	13.832	15.968
	5	1843.920	29.800	∞
K₂	1	165.638	0.000	0.642
	2	81.074	0.642	0.741
	3	185.297	1.383	12.449
	4	2,049.318	13.832	15.968
	5	5,903.836	29.800	∞
K₃	1	179,238	0.000	0.642
	2	47,996	0.642	0.741
	3	42.91	1.383	12.449
	4	277.363	23.832	15.968
	5	2,375.210	29.800	∞
K₄	1	27.224	0.000	0.578
	2	60.464	0.578	0.667
	3	74.877	1.245	11.204
	4	711.592	12.489	14.371
	5	1943.415	26.820	∞
K₅	1	90.646	0.000	0.642
	2	36.267	0.642	0.741
	3	35.609	1.383	12.449
	4	385.650	13.832	15.968
	5	2473.003	29.800	∞
K₆	1	0.032	0.000	0.540
	2	0.094	0.540	0.623
	3	0.428	1.163	10.471
	4	4.628	11.634	13.431
	5	13.142	25.065	11.425
	6	44.961	36.790	∞

In terms of number of geoelectric units or layers, it is seen in Table 11 that there are five layers each for K1, K2, K3, K4, K5 and six layers for K6. The thickest layers of 1597m are those for K1, K2, K3 and K5 and the thinnest layer of 0.54m in the topsoil of K6. The highest resistivity value of 5,903.84Ωm occurs at the fifth layer of K2 and the lowest resistivity value of 0.032Ωm occurs at the top layer of K6. The basement is deepest at K6 and shallowest at K1, K2, K3 and K5.

4.1 Contoured Maps of Layer Resistivity Variation with Depth

In order to look at the areal conductivity of the study area at various depths (levels) of interest, the contour maps of resistivity of the whole area is produced at these levels. Figs 1-7 are maps produced with continuous variations of resistivity values of each multi-layered model beneath the vertical electrical sounding points at the same depth level of interest. Hence, the isopach lines joining points of equal resistivity value at this depth level constitute the contours. This can be viewed from the top as representing the horizontal slicing of the resistivity cubes at these depths. The choice of any contour interval is a function of the clarity with which the contour map can be read and discerned. Usually, the contour intervals are adjusted until a suitable value is determined.

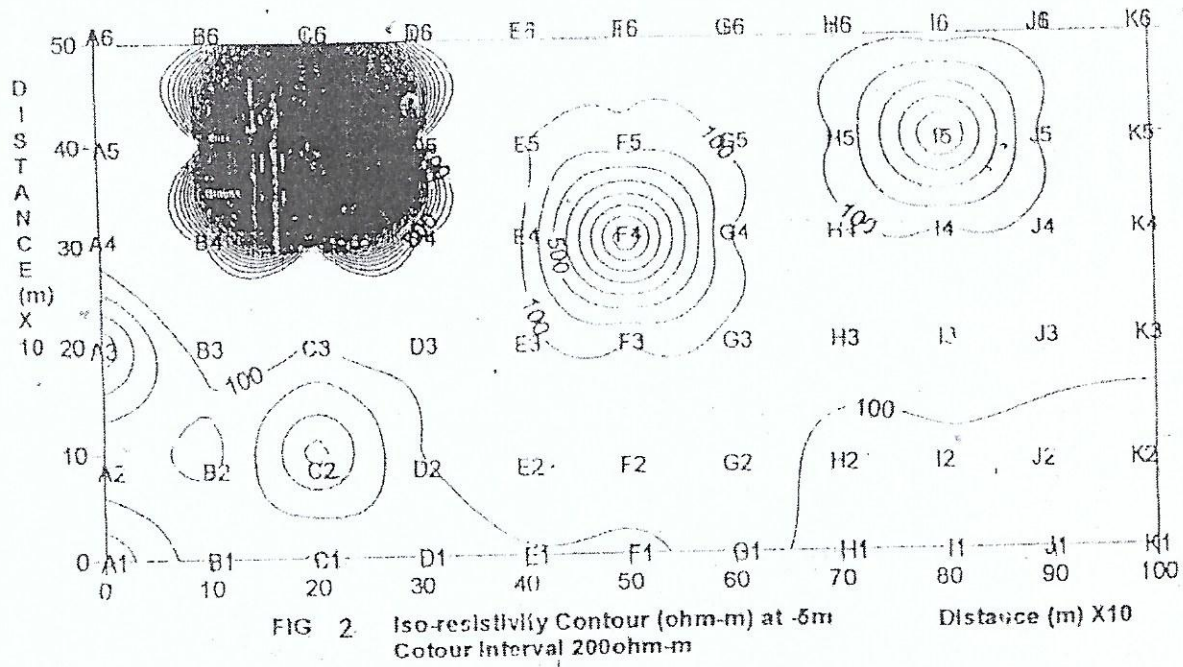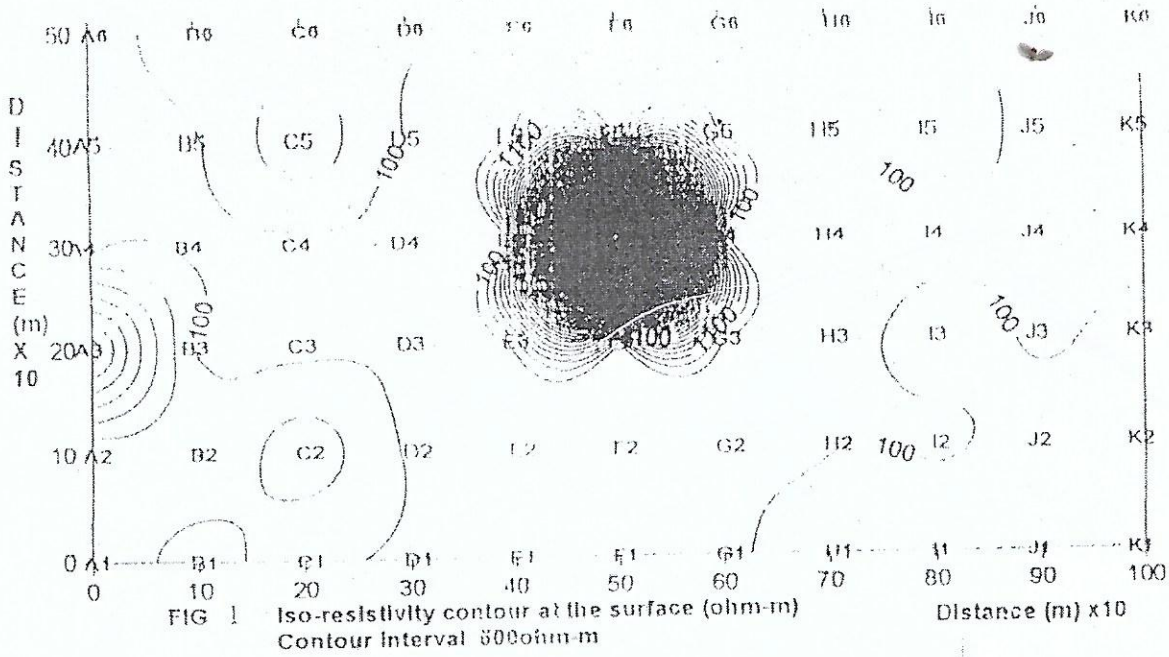### 4.2 Discussion of Iso-Resistivity Maps at Various Depths

Fig. 1 is the resistivity contour map at zero meter depth (i.e the surface); the map was produced at a contour interval of 500 Ωm. The area of very high resistivity value is indicated in this figure in form closures of contour lines around VES station F4 in the central portion of the survey area; it is seen from the figure that VES points E5, F5, G5, G4, G3, F3, E3 and F4 form an outer "envelope" around F4 from which resistivity increase inward towards F4. The western

Geoelectrical Survey for Groundwater at the Gidan Kwano Campus of the Federal University of Technology, Minna- Udensi et al

24

portion of the survey area displays a localized resistivity high around A3 which is differentiated from every other point on the fringe that show general low resistivity anomalies.
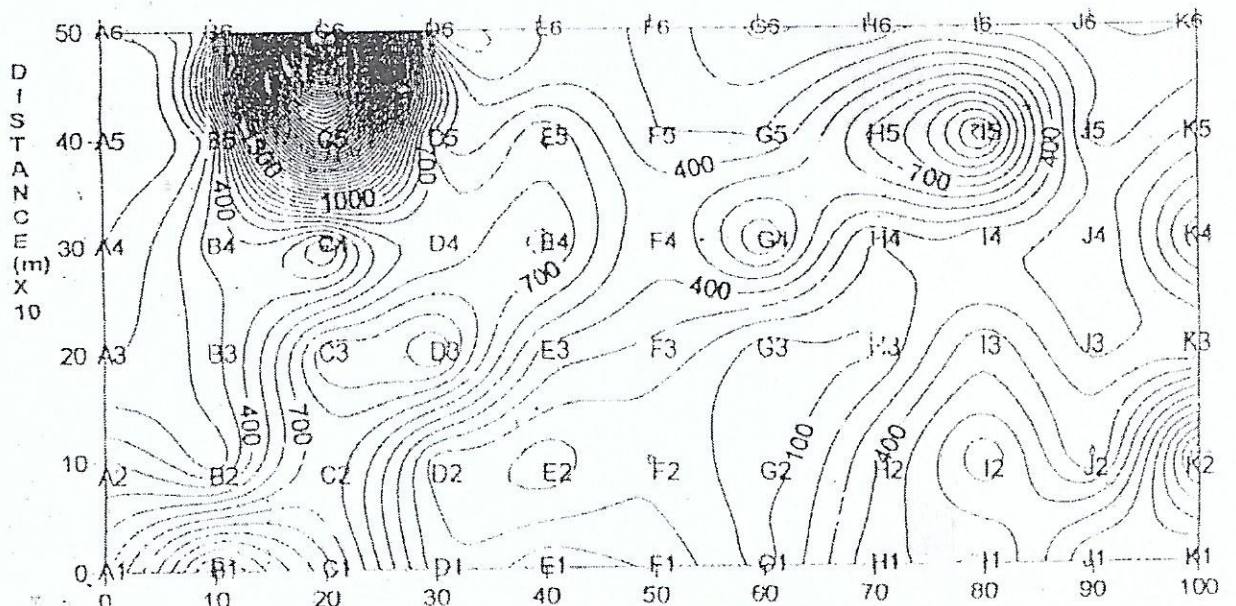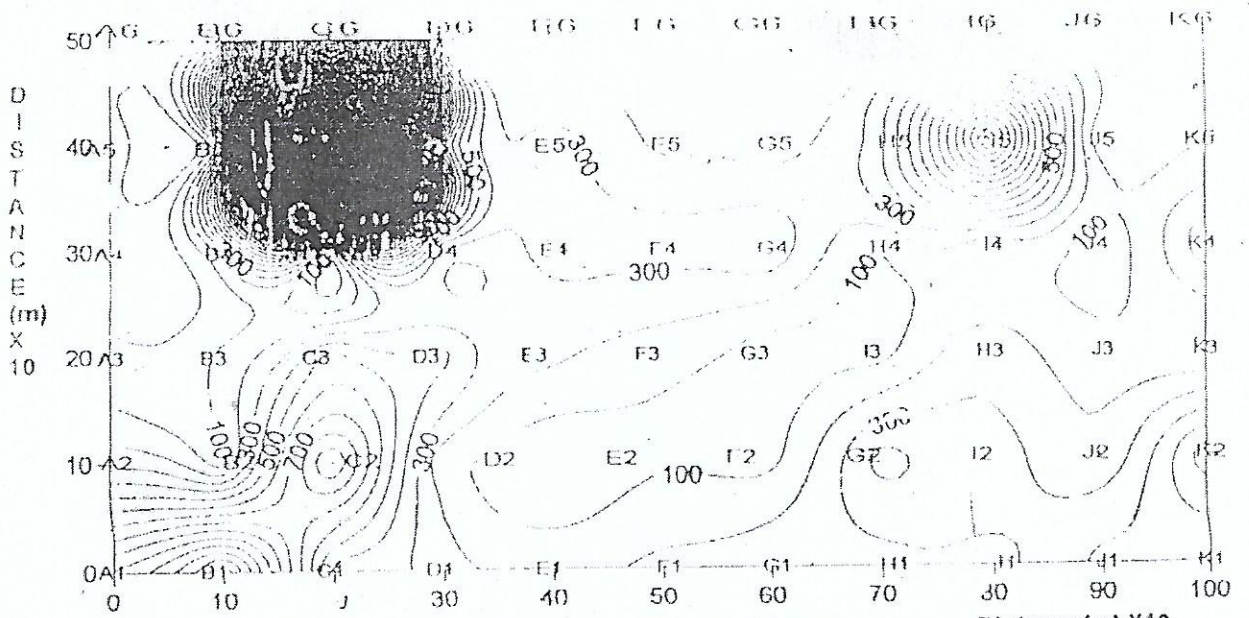
Fig. 2 is the iso-resistivity contour map at the 5m depth; it was produced at 200Ωm contour interval. There is a thick cluster of contour lines centered around VES point C5 in the northwestern part of the survey area. In this map it is seen that VES pants B6, C6, D6, D5, D4, C4, B4, and B5 form an "envelope" around C5. Resistivity increases inward from these points toward C5. The figure also shows contour closures around F4 and I5 that are indicative of high resistivity. Otherwise there is generally a spread of low resistivity portions across the survey area at this depth. A comparison of the surface map and the 5m depth map indicates that the very resistive material around F4 in the surface map has decreased appreciably in the 5m depth map. This may suggest that the material is disappearing or changing composition with depth around F4. Elsewhere the low resistive material at C5 on the surface map has become very resistive on the 5m depth map; this may be interpreted to mean that the material that exhibited just a signature trace on the surface is pronounced at 5m. The same argument can be made for point I5. However, the comparatively high resistive material at A3 on the surface has become somewhat less resistive at the 5m depth.
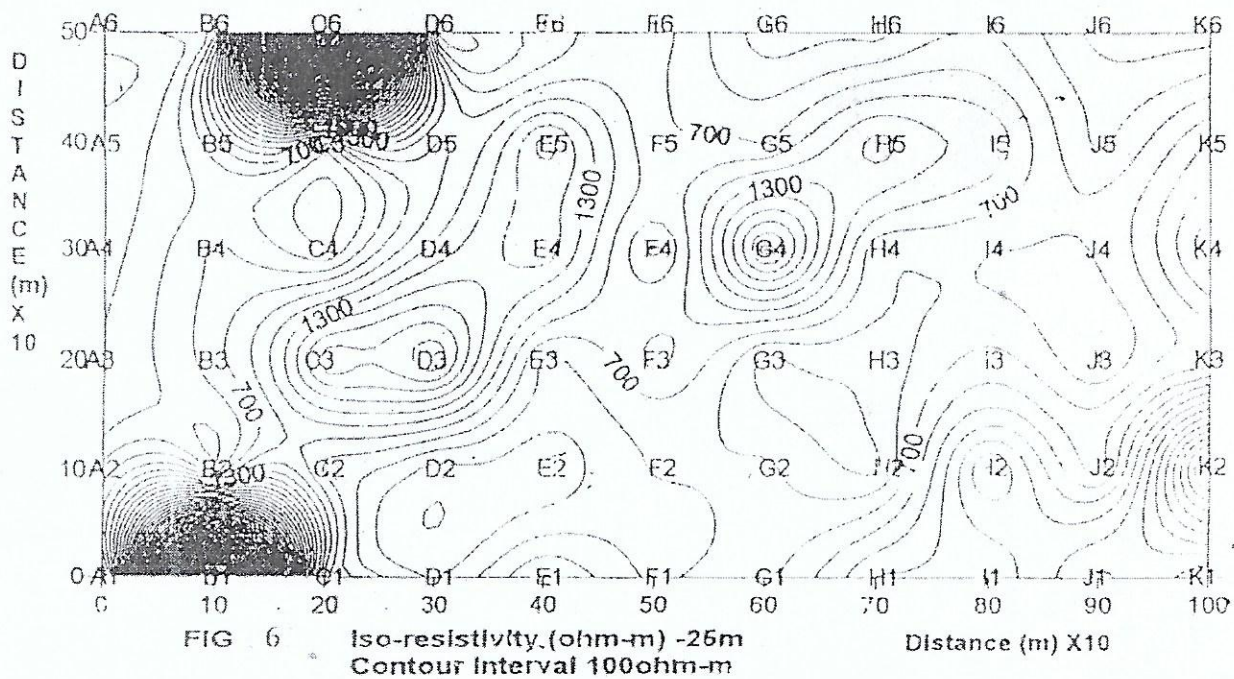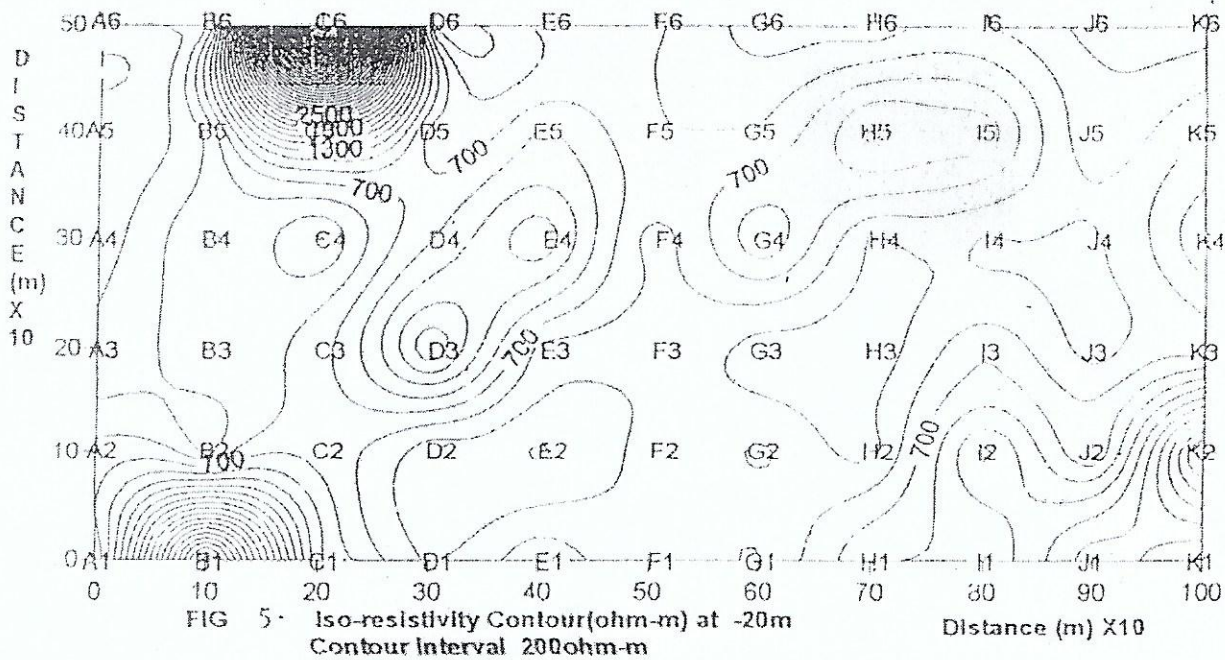
Fig. 3 is the iso-resistivity map for the 10m depth produced using a contour interval of 100Ωm. Thick cluster of contour lines are observed around C5; there is also a closure centered on I5, having a maximum value of 1300Ωm. On the southwestern portion of the survey area there is indication of localized resistivity anomaly of about 900Ωm-1400Ωm around B1 and C2. Elsewhere there is a generally low resistivity regime at the 10m depth. Comparing the 5m and 10m depth maps show the continuation of the very resistive material seen at C5 on the 5m depth map to the 10m depth and an increase in resistivity with depth of the resistivity with depth of the resistive material seen at I5 on the 5m depth map. The resistive material at F4 on the 5m depth map is absent on the 10m depth map. It is instructive to point out that on the surface map, centered on F4, a very resistive material was observed; it can easily be seen that the highly resistive material does not extend down to the 10m point. Furthermore, it is also seen that the material of low resistivity around B1 and C2 on the 5m depth map is characterized by an appreciable jump in resistivity value at the 10m depth map.
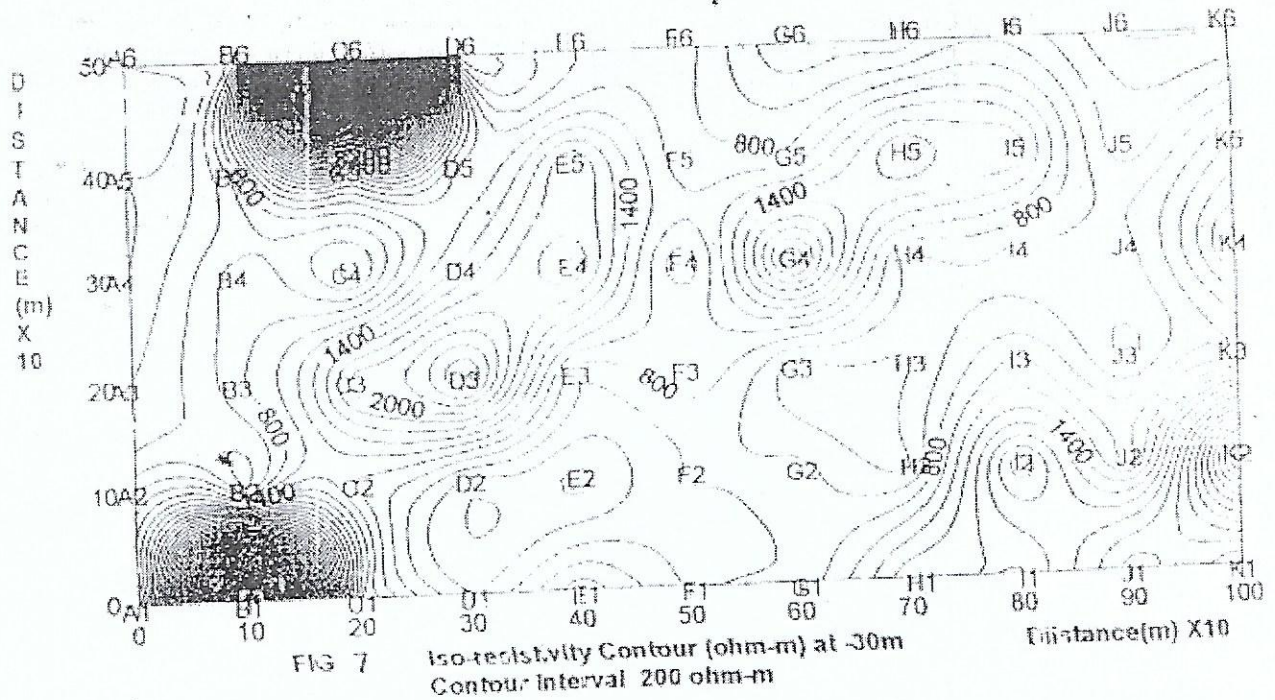
Fig. 4 is the iso-resistivity contour map at the 15m depth part (this map was produced at an interval of 100Ωm); this map shows contour closure around C5. However, the contour cluster has thinned out considerably and the contour label indicates decreasing resistivity values. This structure was identified at the 5m depth map with very thick contour cluster that is indicative of very high resistivity. Elsewhere on the map the material seen at the 10m depth map can be correlated at the 15m depth map with little change in resistivity value, and this can only mean that the composition of the material has not changed much over a vertical distance of 5m. While the resistivity at C5 has decreased for the 15m depth map there is, however, a noticeable jump in resistivity for the other portions of the 15m depth map.

Geoelectrical Survey for Groundwater at the Gidan Kwano Campus of the Federal University of Technology, Minna- Udensi et al

25

FIG 1   Iso-resistivity contour at the surface (ohm-m)
Contour Interval 500ohm-m

FIG 2   Iso-resistivity Contour (ohm-m) at -5m
Cotour Interval 200ohm-m

Geoelectrical Survey for Groundwater at the Gidan Kwano Campus of the Federal University of Technology, Minna- Udensi et al

FIG. 3   Iso-resistivity Contour (ohm-m) at -10m
Contour Interval 100ohm-m

FIG 4   Iso-resistivity Contour(ohm-m) at -15m
Contour interval 100ohm-m

Geoelectrical Survey for Groundwater at the Gidan Kwano Campus of the Federal University of Technology, Minna- Udensi et al

FIG 5. Iso-resistivity Contour(ohm-m) at -20m
Contour interval 200ohm-m

Distance (m) X10

FIG 6 Iso-resistivity (ohm-m) -25m
Contour interval 100ohm-m

Distance (m) X10

Geoelectrical Survey for Groundwater at the Gidan Kwano Campus of the Federal University of Technology, Minna- Udensi et al

FIG 7   Iso-resistivity Contour (ohm-m) at -30m
Contour interval 200 ohm-m

At the 20m depth map (produced at 200Ωm contour interval), Fig.5, the zones of resistivity greater than 200Ωm are beneath VES points C5, B1, and K2. Resistivities in the region of 1500Ωm are found around D3 and E4. There is a generally high resistivity signature spread across the entire profiles at this depth point. Of particular interest is the correlation of the structure at C5 down to the 20m depth. This structure first appeared at the 5m depth point and this would mean that it has no tangible surface signature. The material at B1 is getting reinforced vertically as evidenced from the progressive increase is resistivity value at this 20m depth when compared with the 15m depth point. The material at K2 varies only just slightly.

It is seen in Fig.6, which is the contour map at the 25m depth map (drawn at interval of 100Ωm), that very high resistivities characterize the materials at B1. VES point C5 now lies just on the edge of a highly resistive material whose outer edges are VES B5, B 6, C6, D6, and D5; of course this material correlates very well with the structure that was observed at the 5m depth point all the way down to the 25m depth point. The material around B1, seen at the 20m depth level, has become more resistive at the 25m depth point. Elsewhere on the map there is a localized high resistivity spot around G4, K2, and a dumbbell-shaped spread around C3 and E5 in the west central part of the survey area. The least resistive spot at this depth level does not appear to be less than 700Ωm.

For the iso-resistivity map at the 30m depth level (drawn at a contour interval of 200Ωm) there is, in general, a jump in resistivity value of at least 100Ωm over the 25m depth map, see Fig 7. High resistivity values greater than 3,500Ωm around the northwestern part of the survey area are bounded by VES points B6, C6, D6, D5, C5, and B5. In the extreme southwestern part of the survey area a spot of high resistivity is also bounded by VES points A2, B2, C2, C1, B1, A2, and around K2. The highly resistive material originally centered on C5 that first appeared at the 5m depth map and has been correlated in subsequent depth levels appears to have gradually changed its focus so that at the 20m, 25m and the 30m depth maps the structure is seen to be on around VES point C6. The second highly resistive material seen in this figure is centered on VES point B1; the imprint or signature of this structure was first observed at the 10m depth map. The localized spot around G4 has become highly resistive in the 30m depth map as well as the dumbbell-shaped spread around C3 and E5 in the west central part of the survey area. As was implied earlier, the least resistive spot at this depth does not appear to be less than 800Ωm.

4.3   Discussion of Vertical Cross Section Maps

Figs 8-18 show the maps of the vertical sectioning along each of the eleven profiles. In Fig. 8, the vertical sectioning map for Profile A, a highly resistive material (>1500Ωm) can be found at VES point A3 at about 5m below the ground surface. Another high resistive material of about 100Ωm can be found at VES point A1 at a depth of 10m

Geoelectrical Survey for Groundwater at the Gidan Kwano Campus of the Federal University of Technology, Minna- Udensi et al

29

below the surface. Low resistive regions (usually not greater than 100ohm) occur at VES points A4, A5, and A6 through the range of depths from 0m to 30m. This observation correlates very well with the features seen for the iso-resistivity contour map at zero metre depth (i.e. the surface). In the vertical cross section map for Profile B (Fig.9), there is a region of low resistivity ($\leq 50\ \Omega m$) between VES point B2 and midway to B3 from the surface down to just under the 30m depth point. Resistivity of $\leq 50\Omega m$ can also be observed at the depth of 5m beneath B1; higher resistivity values are noticeable between B1 and B2 as the depth gradually exceeds 5m up to the deepest recorded depth point of 30m. Elsewhere on this profile resistivity values of $> 500\Omega m$ are observed for depth points exceeding 5m.

There is a very high resistive material ($> 15,000$) at VES point C5 that begins manifesting itself from the 5m depth level; the resistivity of this structure falls sharply through the depths, reaching the relatively high value of ≥ 100ohm at the 30m depth point. Profile C (Fig. 10) is characterized in its entirety by resistivity values not usually less than $100\Omega m$, although this $100\Omega m$ region extends to 30m beneath C4. The region between C1 and C5 from surface to 30m depth is characterized by resistivity values of ≤ 2900ohm; the 2900ohm occurs at about 30m beneath C3.
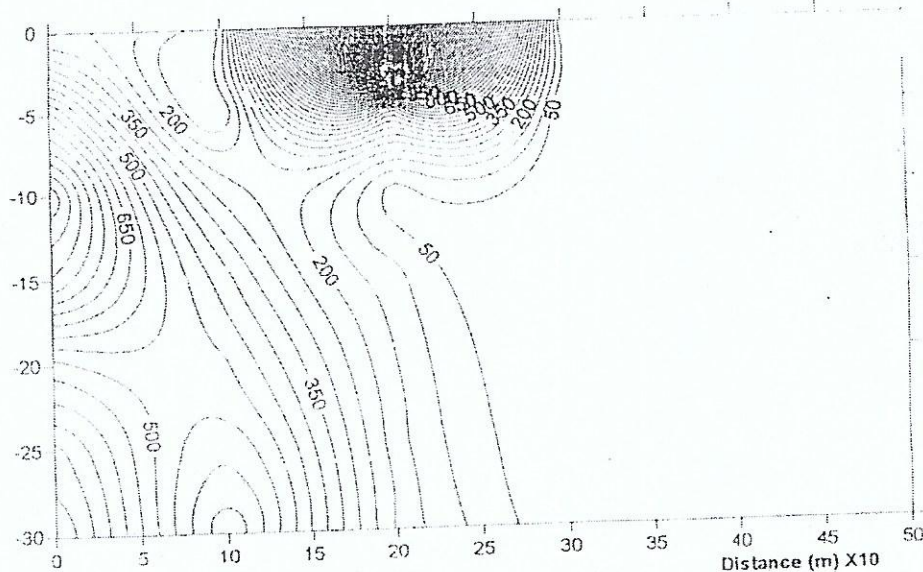

FIG 8   Vertical Sectioning for A Profile
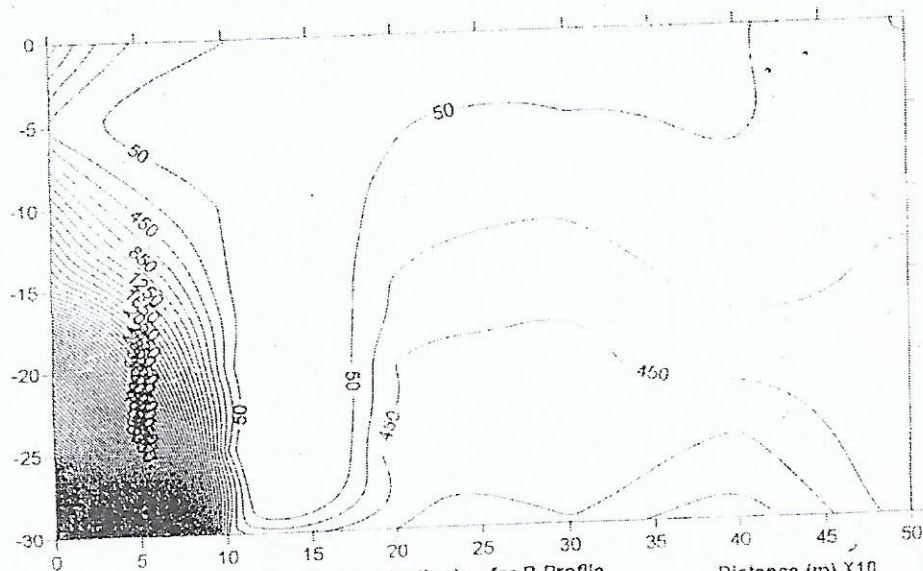Contour Interval 50ohm-m

FIG 9   Vertical Sectioning for B Profile
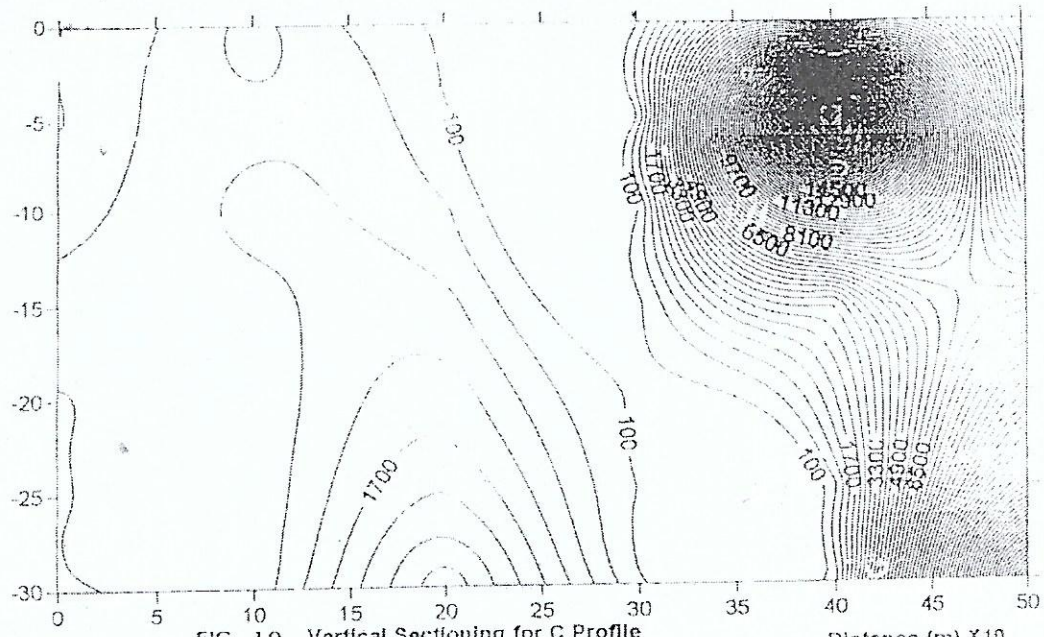Contour Interval 200ohm-m

FIG. 10   Vertical Sectioning for C Profile
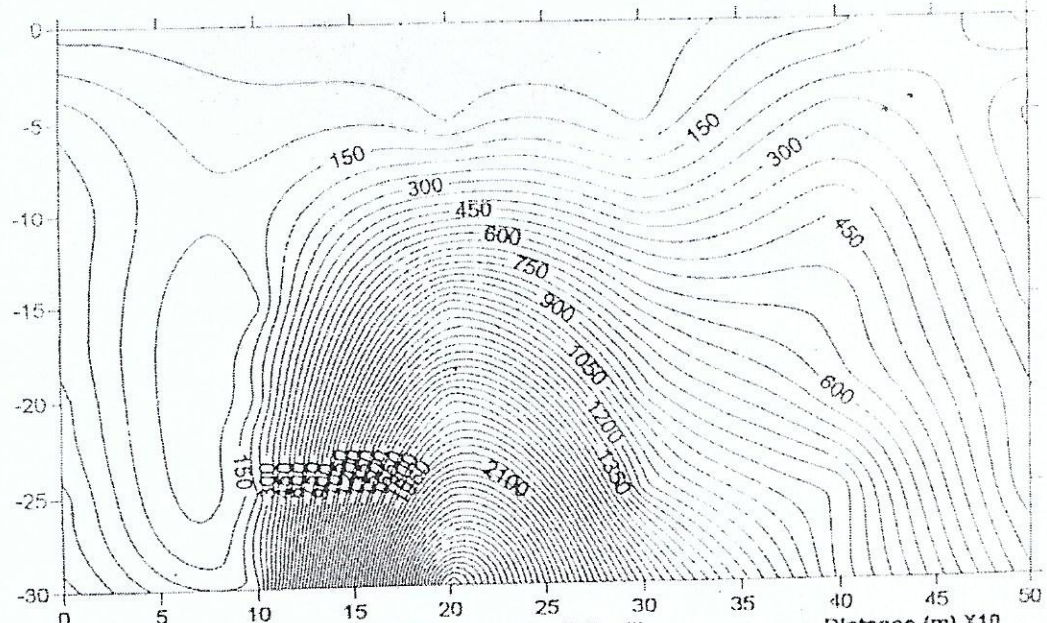Contour Interval 400ohm-m

Distance (m) X10

FIG. 11 Vertical Sectioning for D Profile
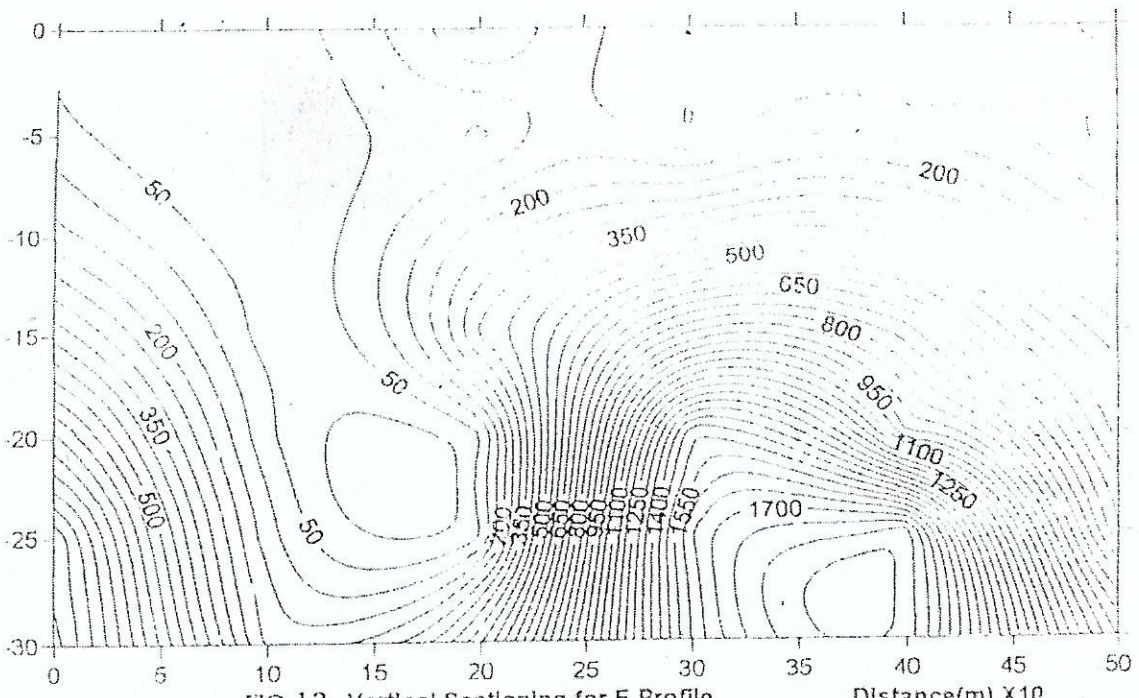Contour Interval 50m

Distance (m) X10

Geoelectrical Survey for Groundwater at the Gidan Kwano Campus of the Federal University of Technology, Minna- Udensi et al

FIG.12   Vertical Sectioning for E Profile
Contour Interval 50m

Distance(m) X10

FIG 13   Vertical Sectioning for F Profile
Contour Interval 200m
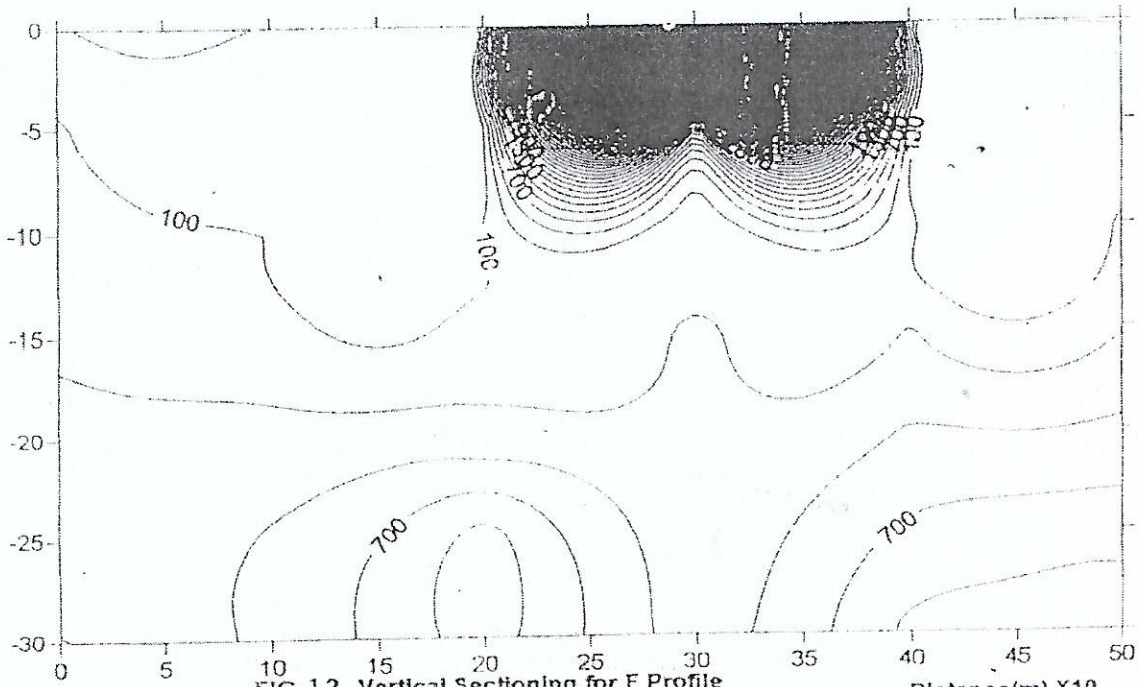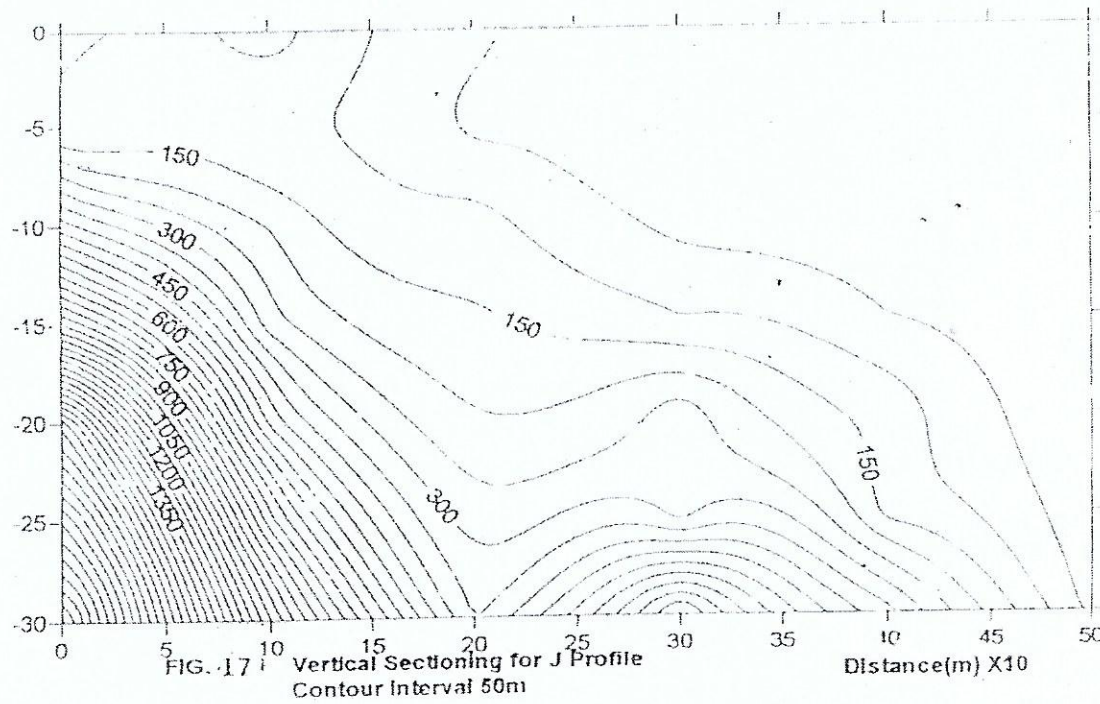
Distance(m) X10

Geoelectrical Survey for Groundwater at the Gidan Kwano Campus of the Federal University of Technology, Minna- Udensi et al

FIG. 14 Vertical Sectioning for G Profile
Contour Interval 100m

FIG. 15 Vertical Sectioning for H Profile
Contour Interval 50m

Geoelectrical Survey for Groundwater at the Gidan Kwano Campus of the Federal University of Technology, Minna- Udensi et al

FIG.16 Vertical Sectioning for I Profile
Contour Interval 100m
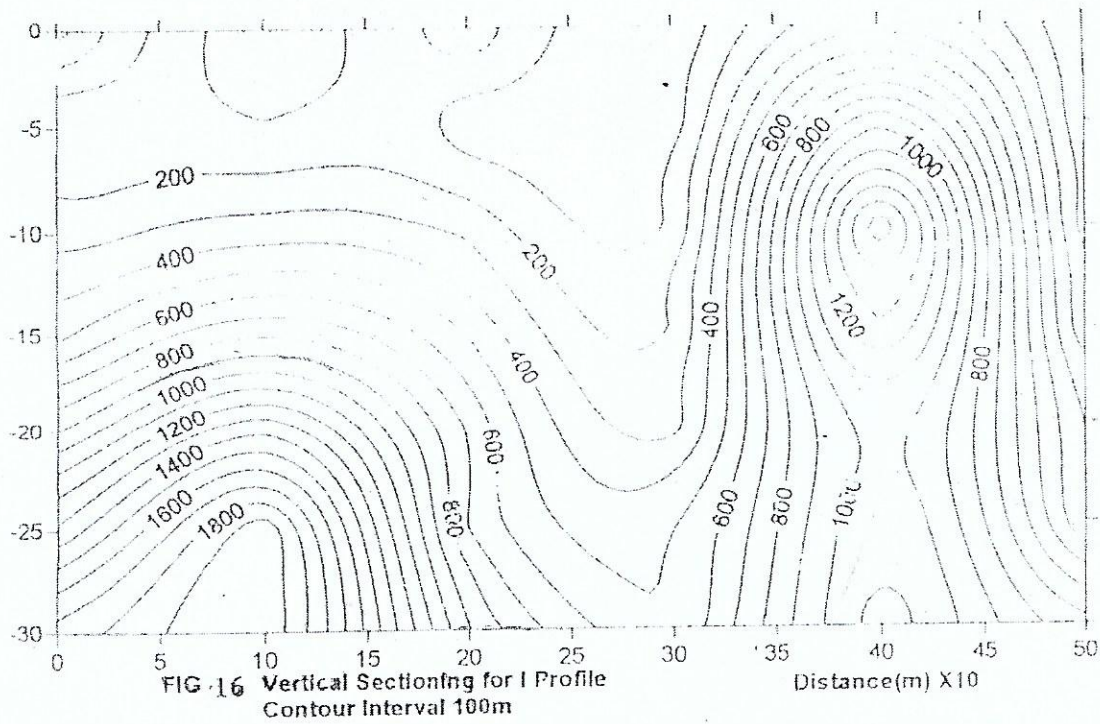

FIG. 17 Vertical Sectioning for J Profile
Contour Interval 50m

Geoelectrical Survey for Groundwater at the Gidan Kwano Campus of the Federal University of Technology, Minna- Udensi et al
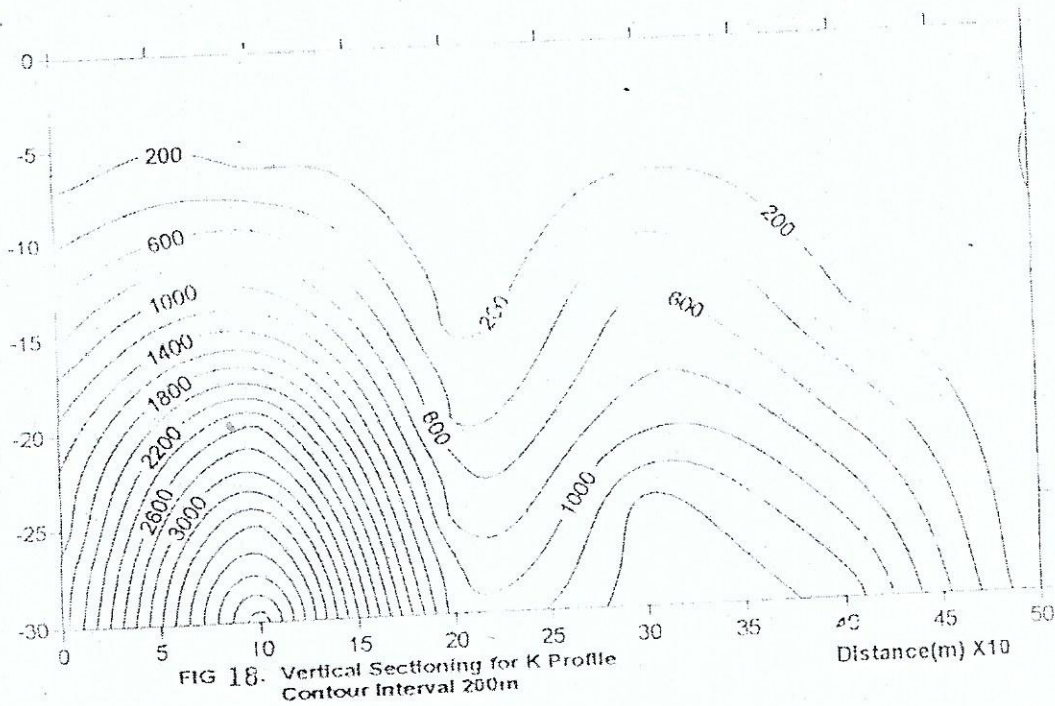
FIG 18. Vertical Sectioning for K Profile
Contour Interval 200m

In the map for the vertical cross section for profile D (Fig. 11), there is no discernible region having a resistivity of about 50Ωm for the entire depth surveyed, however, the region between D1 and D2 is characterized by a resistivity region having values of 150Ωm-350Ωm up to 30m deep. In the map for the vertical cross section for Profile E (Fig. 12), the maximum discernible value of resistivity is 1850Ωm and this occurs between VES points E4 and E5 at close to the 30m depth. Between 15m and 30m depths on the linear stretch between E2 and E3 the resistivity of the zone lies between 50Ωm and 200Ωm. A resistivity zone of 200Ωm at 15m depth point exists between E1 and E2.

In the map for the vertical cross section for Profile F (Fig. 13), near homogenous or stratified continuous resistivity zones can be observed from about 100Ωm at the 10m depth level through 300Ωm at the 17m depth level, 500Ωm at the 23m depth level, 700Ωm at the 25m depth level, and 900Ωm at the 28m depth level. The vertical cross section for Profile G (Fig. 14) shows a feature that approximates a trough or synclinal structure having resistivity values between 100Ωm and 500Ωm underneath G3; the structure can be mapped from the 15m depth point through to the 30m depth point. Low resistivity region from the surface to the maximum surveyed depth of 30m can be identified between VES points E5 and E6.

The map for the vertical cross section for Profile H (Fig. 15) shows regions of relatively low resistivities overall. The region between H2 and H4 is characterized by a maximum resistivity value of 550Ωm underneath E3 at the 30m depth point while a stretch of 50Ωm end 250Ωm can be identified between the 10m and the 25m depth levels. In the map for the vertical profile of Profile I (Fig. 16), a material that does not vary too much in composition is seen to exhibit a maximum resistivity of less than 600Ωm from the surface to the 30m depth level beneath VES point I4. Overall, the region beneath VES point I3 and I5 (I4 inclusive) from the surface to well below the 30m point is characterized by relatively low resistivity values of not more that 1100Ωm.
The vertical cross section map for Profile J (Fig. 17) shows a 150-350Ωm region between 10m and 30m beneath J3, a 50-350Ωm region between 15m and 30m on the linear stretch between J5 and J6. In the vertical cross section map for Profile K (Fig. 18), a 200Ωm "envelope" at 15m underneath K3, 7m underneath K4, and up to 30m underneath K6 is observed for Profile K. Beneath this "envelope" there is a proportional increase in resistivity with depth, up to a maximum of 4400Ωm underneath K2.

4.4   The Aquiferous Horizon
There are about three main factors that determine the areas suitable for groundwater exploitation. These factors are the conductivity of the subsurface, the presence of suitable aquifer, and the thickness of the aquifer. From the above factors, zones or areas that will be considered to be suitable for groundwater exploitation form the weathered basement

which is the major component of any aquifer system. The aquifer system in the basement areas consists of weathered and fractured basement. Where the fractured zone is saturated, relatively high groundwater can be sustained from borehole penetrating such a sequence (Salako and Udensi, 2005).

5.0   Conclusion and Recommendation

The analysis of the data and curves reveal the presence of four to six subsurface geoelectric units or layers underneath these sections. The thickness and resistivity values of the different layers were determined from the VES data. The layers that were identified correspond to lateritic topsoil, fadama loam, sandy clay, sand gravel, weathered basement, fractured basement, and fresh basement. The vertical cross section maps reveal features that resemble synclinal and anticlinal structures. The anticlinal features imply relatively thin overburden cover while the synclinal features imply depressions or buried valleys that are characterized by relatively thick overburden level. It can be deduced from the works of Shuaibu et al (2004), Salako and Udensi (2005) that the synclinal features that are characterized by very thick overburden cover are prospects for groundwater accumulation. Furthermore it can be inferred from the work of Salako and Udensi (2005) that a minimum overburden thickness of 15m over the weathered and fractured basement would suffice to form an aquifer.

In this work the necessity to identify possible aquifers at the weathered and fresh basement is justified on the earlier work of Salako and Udensi (2005). Because of the proximity of the survey area of Salako and Udensi (2005) to the location of the present study and owing to the geological homogeneity of both survey areas, it is very conceivable that the aquiferous zones identified in Salako and Udensi (2005) would be an integral component of the entire groundwater aquifer resource complex of the Gidan Kwano Campus of the Federal University of Technology, Minna. In this research work the VES points that are characterized by groundwater potential at the suitably surveyed depths are A3 – A5, B2 – B6, C1 – C2, C4 – C5, DI – D2, D5 – D6, E2 – E3, E4 – E5, F1 – F6, G2, G5 – G6, H2 – H4, I3 – I6, J3 – J6, K3 – K6. However, the VES points that are underlain by thick overburden and are thus recommended for drilling for water exploitation are B2, C4, E2, G3, I4, J3, J6, K3 and K6.

References

Ako, B.J. and Olorunfemi, M.O. (1982). Geoelectric survey for groundwater in the New Basalt of Vom, Plateau State. *Journal of Mining and Geology*, 8(2), 273-280.

Bhattacharya, B.B. (1986). Advances in Geophysics, Oxford and IBH Publishing, New Delhi.

Bonde, D.S. (1997). Geoelectrical survey for groundwater resources in Egba, Shiroro Local Government Area, Niger State, M.Tech. dissertation, Federal University of Technology, Minna.

Dangana, L.M. (2002). Electrical resistivity survey of Tunga Kawo Dam, Wushishi, Niger State, Nigeria, M.Tech. dissertation, Federal University of Technology, Minna.

Gana, J.S. (1995). Geophysical exploration for groundwater in Yakila, Niger State, M.Tech. dissertation, Federal University of Technology, Minna.

Kearey, P. and and Brooks, M. (1988). *Fundamentals of Geophysics*, Cambribge University Press, Cambridge.

Okwueze, E.E. and Ezeanyi, V. (1985). The vertical electrical sounding (VES) method in laterite region and iron-rich area. Journal of Mining and Geology, 22 (1 and 2), 173-280.

Okwueze, E.E., Ebeniro, J.O., and Mbogning, M. (1981). The geoelectric structure of Lake Nyos Dam, Cameroon, and its geoelectric implication. *Journal of Mining and Geology*, 8(2), 273-280.

Olorunfemi, M.O. and Fasuyi, S. A. (1993). Aquifer types and the geoelectric/hydrogeological characteristics of part of the Central Basement Terrain of Nigeria (Niger State). Journal of African Earth Sciences, 16(3), 309-317.

Olorunfemi, M.O. and Okhue, E.T. (1992). Hydrogeological and geological significance of geoelectric survey at Ile-Ife. *Nigerian Journal of Mining and Geology*, 28(2), 221-228.

Parasnis, D.S. (1988). Principles of Applied Geophysics (4ed.), Chapman and Hall, London.

Salako, K.A. and Udensi, E.E. (2005). Vertical electrical sounding investigation of western part of the Federal University of Technology, Gidan Kwano Campus, Minna. *Proc: First Annual S.S.S.E. Conference (F.U.T. Minna)*, 1, 69-78.

Shuaibu, O.Y., Udensi, E.E., Adeniyi, J.O., and Jonah, S.A. (2004). Resistivity survey of the western part of Plateau State Polytechnic Permanent Site, Barkin Ladi, Nigeria. *Zuma Journal of Pure and Applied Sciences*, 6(2), 160 –167

Udensi, E.E., Ogunbajo, M.I., Nwosu, J.E., Jonah, S.A., Kolo, M.T., Onoduku, U.U., Crown, I.E., Daniyan, M.A., Adeniyi, J.O., and Okosun, F.A. (2005). Hydrogeological and geophysical surveys for groundwater at designated premises of the main campus of the Federal University of Technology, Minna. *Zuma Journal of Pure and Applied Sciences*, 7(1), 52-58.

Zohdy, A.A.R. (1989). A new method for the automatic interpretation of Schlumberger and Wenner sounding curves. *Geophysics*. 54(2), 245-253.

Geoelectrical Survey for Groundwater at the Gidan Kwano Campus of the Federal University of Technology, Minna- Udensi et al

36

169

APPENDICES

A. Complete Dataset for Profiles A-K

Table A1: Dataset for Profile A

MN/2 (m)	Geo FAC	A_1R (Ω)	RES (Ωm)	A_2R (Ω)	RES (Ωm)	A_3R (Ω)	RES (Ωm)	A_4R (Ω)	RES (Ωm)	A_5R (Ω)	RES (Ωm)	A_6R (Ω)	RES (Ωm)
1	2.36	31.4	73.4904	72.24	170.486	66.47	156.869	5.5	12.98	62.91	148.468	48.47	114.389
2	11.8	2.84	33.51	6.1	71.98	7.62	89.916	1.37	16.166	0.91	10.738	11.07	130.62(
3	27.8	7.78	216.284	1.29	35.862	2.26	62.828	0.66	18.348	1.14	31.692		27.8
5	77.8	0.348	27.0744	0.65	50.57	1.25	97.25	0.35	27.23	0.404	31.4312	1.1	85.58
6	112	1.32	147.84	1.32	147.84	0.428	47.936	0.202	22.624	0.122	13.664	0.663	74.256
6	55	0.773	12.515	1.57	86.35	0.691	38.005	1.31	72.05	0.658	36.19	16.34	898.7
8	99	0.568	8.232	0.8	79.2	0.551	54.549	0.395	39.105	0.55	54.45	45.88	4542.1:
10	156	0.255	39.78	0.526	82.056	0.144	22.464	0.033	5.142	0.848	132.288	4.44	692.64
10	58	0.848	49.184	1.02	59.16	2.16	125.28	0.129	7.482	0.514	29.812	1.08	62.64
15	137	0.59	80.83	0.633	86.721	0.162	22.194	0.964	132.068	0.275	37.675	1.11	152.07
20	245	0.331	81.095	0.389	95.305	0.046	11.27	0.259	63.455	0.184	45.08	0.87	213.15
30	562	0.189	106.218	0.222	124.764	0.103	57.886	0.977	549.074	0.056	30.19	0.366	205.69:
40	1001	0.01	10.01	0.1777	177.177	0.042	42.042	0.083	83.083	4.84	4844.84	4.74	4744.7
40	323	0.517	166.991	0.55	1777.65	0.52	167.96	0.102	32.946	0.319	103.037	5.5	1776.5
50	512	0.485	248.32	0.398	201.216	0.279	142.848	0.142	75.264	0.238	121.856	0.938	480.25(
60	742	0.377	279.734	0.416	308.672	0.242	179.564	0.12	89.04	0.269	199.598	1.2	890.4
70	1914	0.207	209.898	0.267	270.738	0.184	186.286	0.625	633.75	0.259	262.626	28.19	28584.
80	1329	0.236	313.644	0.157	208.653	0.163	216.627	1.33	1767.57	0.077	102.333	6.65	8837.8:
80	647	0.574	371.387	0.416	269.152	0.329	212.863	0.239	154.633	0.213	137.811	1.9	1229.3
90	825	0.457	378.675	0.385	317.625	0.287	236.775	0.222	183.15	0.227	187.275	4.9	4042.5
100	1024	0.382	391.168	0.384	290.816	0.196	200.704	0.204	208.896	0.215	220.16	0.725	742.4

Table A2: Dataset for Profile B

IN/2 (m)	Geo FAC	B₁R (Ω)	RES (Ωm)	B₂R (Ω)	RES (Ωm)	B₃R (Ω)	RES (Ωm)	B₃R (Ω)	RES (Ωm)	B₃R (Ω)	RES (Ωm)	B₄R (Ω)	RES (Ωm)
	2.36	206	486.16	131.86	311.19	5.67	13.3812	24.43	57.6548	39.34	92.8424	19.07	45.0052
	11.8	17.89	211.102	13.87	163.666	1.99	23.482	0.806	9.5108	3.59	42.362	2.75	32.45
	27.8	6.36	176.808	4.08	113.424	1.89	28.634	7.66	212.948	1.34	37.252	1.45	40.31
	77.8	2.08	161.824	1.61	125.258	0.43	33.454	3.87	301.088	0.463	36.0214	0.515	40.067
	112	1.3	145.6	1.04	116.48	0.327	36.624	16.24	1825.88	0.349	39.088	1.41	157.92
	55	2.89	158.95	1.75	96.25	0.75	41.25	0.725	39.875	0.374	20.57	1.12	61.6
	99		99	1.39	137.61	0.589	58.311	0.608	60.192	0.493	48.807	0.755	74.745
0	156	1.73	269.88	1.04	157.56	398	62.088	0.0724	11.2944	0.364	56.784	0.328	51.168
0	58	3.6	208.8	2.75	159.5	0.858	49.764	3.95	229.1	0.931	53.998	42.37	2457.46
5	137	1.7	232.9	1.52	208.24	0.428	58.636	0.373	51.101	0.517	70.829	0.36	49.32
20	245	1.36	333.2	0.923	226.135	0.382	93.59	1.81	443.45	0.358	87.71	1.82	445.9
	562	2.4	1348.8	0.455	255.71	0.238	133.756	0.157	88.234	0.209	117.458	0.73	410.26
40	1001	0.525	525.525	13.3	13313.3	0.176	176.176	4.08	4084.08	0.226	226.226	0.237	237.237
	323	0.281	90.763	0.843	272.289	0.379	122.417	64	20672	0.402	129.846	0.725	234.175
50	512	22.6	11571.2	0.616	315.392	0.313	160.256	1.27	650.24	0.299	153.088	0.685	350.72
50	742	0.097	71.974	0.349	258.954	0.231	171.402	99.57	73880.9	0.239	177.338	0.451	334.642
70	1914	2.06	2088.84	0.281	284.934	0.207	209.898	6.93	7027.02	0.244	247.416	0.477	483.678
80	1329	0.296	393.384	0.352	467.808	0.196	260.484	1.28	1701.12	0.227	301.683		1329
80	647	6.01	3888.47	6.56	4244.32	0.37	239.39	0.894	578.418	0.382	247.154	1.23	795.81
90	825	1.92	1584	0.656	541.2	0.356	293.7	23.8	19635	0.397	327.525	1.6	1320
100	1024	1.68	1720.32	73.7	75468.8	0.339	347.136	4.42	4526.08	0.419	429.056	0.545	558.08

Geoelectrical Survey for Groundwater at the Gidan Kwano Campus of the Federal University of Technology, Minna- Udensi et al

38